

# Novel fully protected muramic acid: A facile synthesis and structural study



Monika Kovačević<sup>a</sup>, Vladimir Rapić<sup>a</sup>, Iva Lukač<sup>a</sup>, Krešimir Molčanov<sup>b</sup>, Ivan Kodrin<sup>c</sup>, Lidija Barišić<sup>a,\*</sup>

<sup>a</sup> Department of Chemistry and Biochemistry, Faculty of Food Technology and Biotechnology, Pierottijeva 6, HR-10000 Zagreb, Croatia

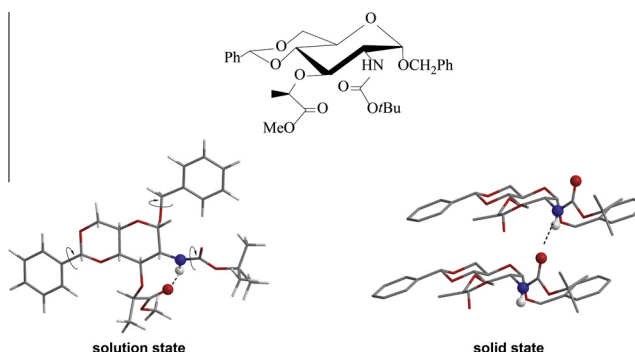
<sup>b</sup> Division of Physical Chemistry, Ruđer Bošković Institute, Bijenička cesta 54, HR-10000 Zagreb, Croatia

<sup>c</sup> Department of Chemistry, Faculty of Science, Horvatovac 102a, HR-10000 Zagreb, Croatia

## HIGHLIGHTS

- *N*-Ac-Mur-OMe is transformed into *N*-Boc-Mur-OMe.
- Eight membered NH...OC<sub>ester</sub> intramolecular hydrogen bond is preserved in solution upon alteration of protecting group.
- Intermolecular hydrogen bonding occurs in the solid-state of *N*-Boc-Mur-OMe.

## GRAPHICAL ABSTRACT



## ARTICLE INFO

### Article history:

Received 21 March 2013  
Received in revised form 5 June 2013  
Accepted 5 June 2013  
Available online 12 June 2013

### Keywords:

Protected muramic acid  
Structural analysis  
X-ray crystallography  
DFT calculations

## ABSTRACT

Synthesis and structural characterisation of novel fully protected muramic acid **2** (*N*-Boc-Mur-OMe, Mur = muramic acid) has been reported. *N*-Ac-Mur-OMe (**1**) prepared starting from commercially available *N*-acetylglucosamine, was treated with di-*tert*-butyl dicarbonate (Boc<sub>2</sub>O) and *N,N*-dimethyl-4-aminopyridine (DMAP) in tetrahydrofuran. The intermediate mixed imide *N*-Ac-*N*-Boc-Mur-OMe was converted to *N*-Boc-Mur-OMe (**2**) upon *in situ* treatment with hydrazine hydrate in methanol. The structural analysis of **2**, performed by IR and NMR spectroscopic methods and X-ray crystallography, was augmented by computational calculations including molecular and density functional theory studies (DFT) using M06/6-31G(d) computational model. The spectroscopic and DFT data obtained for novel Boc-protected **2** were compared with corresponding experimental values of its previously described Ac-protected analogue **1** in order to examine if the replacement of the protecting groups influences the conformational properties.

© 2013 Elsevier B.V. All rights reserved.

## 1. Introduction

Muropeptides are degradation products of peptidoglycans that contain muramic acid (Mur) coupled to amino acids. They are known as biologically active compounds, e.g. they exhibit increased immunoadjuvant activity [1].

The structural properties of bioorganometallic muropeptides **I** [*N*-Ac-Mur-Ala-Fca; Fca = 1'-aminoferrocene-1-carboxylic acid] and **II** [*N*-Ac-Mur-NH-Fn-R; Fn = 1,1'-ferrocenylene, R = H (**IIa**), COOMe (**IIb**), NHAc (**IIc**)] have already been investigated in our group [2,3] (Fig. 1). The detailed structural studies in solution confirmed strong influence of ferrocene moiety on conformational properties of **I** and **II**. Moreover, the cyclic voltammograms of **II** featured a one-electron oxidation for the ferrocene/ferrocenium redox couple. Furthermore, Fca-containing peptides with Ala were

\* Corresponding author. Tel.: +385 1 46 05 069; fax: +385 1 48 36 082.  
E-mail address: [lbaris@pbf.hr](mailto:lbaris@pbf.hr) (L. Barišić).



72%) were obtained. Mp 158.7–163.7 °C;  $R_f = 0.6$  (hexane:ethylacetate = 3:1); IR ( $\text{CH}_2\text{Cl}_2$ ,  $\text{cm}^{-1}$ ):  $\nu$  3431(w,  $\text{NH}_{\text{free}}$ ), 3356 (m,  $\text{NH}_{\text{assoc}}$ ), 1732 (s,  $\text{CO}_{\text{ester}}$ ), 1709 (s,  $\text{CO}_{\text{Boc}}$ ).  $^1\text{H}$  NMR ( $\text{CDCl}_3$ , 300 MHz):  $\delta$  (ppm) 7.45–7.25 (m, 10H,  $\text{CH}_{\text{Ph}}$ ), 6.02 (d, 1H,  $J = 5.1$  Hz, NH), 5.56 (s, 1H,  $\text{CH}_{\text{benzylidene}}$ ), 5.27 (d, 1H,  $J = 2.6$  Hz, H-1), 4.68 (d, 1H,  $J = 12.0$  Hz,  $\text{OCH}_{2\text{a-Ph}}$ ), 4.55 (d, 1H,  $J = 12.0$  Hz,  $\text{OCH}_{2\text{b-Ph}}$ ), 4.50 (q, 1H,  $J = 6.8$  Hz,  $\text{CH}_{\text{Lac}}$ ), 4.19 (dd, 1H,  $J = 4.2$  Hz,  $J = 9.5$  Hz, H-3), 3.84–3.81 (m, 1H, H-4), 3.79 (d, 1H,  $J = 9.6$  Hz, H-6b), 3.73 (d, 1H,  $J = 9.6$  Hz, H-6a), 3.72 (brs, 4H,  $\text{OCH}_3 + \text{H-2}$ ), 3.65 (pt, 1H, H-5), 1.45 (s, 9H,  $\text{C}(\text{CH}_3)_3$ ), 1.40 (d, 3H,  $J = 6.9$  Hz,  $\text{CH}_3\text{-Lac}$ );  $^{13}\text{C}$  NMR ( $\text{CDCl}_3$ , 75 MHz):  $\delta$  (ppm) 174.48 ( $\text{CO}_{\text{ester}}$ ), 156.14 ( $\text{CO}_{\text{Boc}}$ ), 137.38, 137.31 ( $\text{C}_{\text{Ph}}$ ), 128.99–125.87 ( $\text{CH}_{\text{Ph}}$ ), 101.27 ( $\text{CH}_{\text{benzylidene}}$ ), 97.59 ( $\text{C}_1$ ), 83.33 ( $\text{C}_5$ ), 79.14 ( $\text{C}(\text{CH}_3)_3$ ), 75.34 ( $\text{CH}_{\text{Lac}}$ , C3), 70.05 ( $\text{CH}_2\text{Ph}$ ), 69.02 (C6), 62.83 (C4), 54.92 (C2), 52.09 ( $\text{OCH}_3$ ), 28.43 ( $\text{C}(\text{CH}_3)_3$ ), 18.78 ( $\text{CH}_3\text{-Lac}$ ). Anal. Calcd. [ $\text{C}_{29}\text{H}_{37}\text{N}_1\text{O}_9$ ]: C 64.07, H 6.86, N 2.58%; Found: C 64.04, H 6.89, N 2.56%.

### 2.3. Determination of crystal structure

Crystals suitable for data collection were grown from ethanol by vapour diffusion at low temperature (4 °C). Single crystal measurement was performed on an Oxford Diffraction Xcalibur Nova R (CCD detector, microfocus Cu tube) at room temperature [293(2) K]. Since the absolute configuration was known from the synthetic procedure, only the symmetry-independent part of the Ewald sphere was measured. Program package CrysAlis PRO [9] was used for data reduction. The structures were solved using SHELXS97 [10] and refined with SHELXL97 [10]. The models were refined using the full-matrix least squares refinement; all non-hydrogen atoms were refined anisotropically. Hydrogen atoms were treated as constrained entities, using the command AFIX in SHELXL97 [10]. Molecular geometry calculations were performed by PLATON [11], and molecular graphics were prepared using ORTEP-3 [12], and CCDC-Mercury [13]. Crystallographic and refinement data for the structures reported in this paper are shown in Table 1.

**Table 1**  
Crystallographic, data collection and structure refinement details.

Compound	<b>N-Boc-Mur-OMe (2)</b>
Empirical formula	$\text{C}_{29}\text{H}_{37}\text{N}_1\text{O}_9$
Formula (wt./g mol $^{-1}$ )	543.60
Crystal dimensions (mm)	$0.15 \times 0.04 \times 0.03$
Space group	$P 2_1 2_1 2_1$
$a$ (Å)	5.10930(10)
$b$ (Å)	21.2302(5)
$c$ (Å)	26.6982(5)
$\alpha$ (°)	90
$\beta$ (°)	90
$\gamma$ (°)	90
$Z$	4
$V$ (Å $^3$ )	2895.99(10)
$D_{\text{calc}}$ (g cm $^{-3}$ )	1.247
$\mu$ (mm $^{-1}$ )	0.765
$\Theta$ range (°)	3.31–76.15
$T$ (K)	293(2)
Diffractometer type	Xcalibur Nova
Range of $h, k, l$	$-6 < h < 4$ $-26 < k < 24$ $-32 < l < 33$
Reflections collected	9515
Independent reflections	5409
Observed reflections ( $I \geq 2\sigma$ )	4621
Absorption correction	Multi-scan
$R_{\text{int}}$	0.0220
$R$ ( $F$ )	0.0816
$R_w$ ( $F^2$ )	0.2566
Goodness of fit	1.045
H atom treatment	Constrained
No. of parameters, restraints	351, 20
$\Delta\rho_{\text{max}}, \Delta\rho_{\text{min}}$ (eÅ $^{-3}$ )	0.724; -0.409

### 2.4. Theoretical methods

The initial monomer geometry of *N*-Boc-Mur-OMe (**2**) was cut out from the X-ray determined structure. The conformational analysis was performed with MacroModelv9.8 [14] molecular modelling program applying different search methods and force fields. The class of the most stable conformers thus obtained, was optimized with the three different functionals (B3LYP, M06 and M06-2X) and 6-31G(d) basis set in vacuum and implicitly modelled chloroform (using polarizable continuum model, PCM). Vibrational frequencies were calculated to verify true minima on the potential energy surface. All quantum mechanical calculations were performed with Gaussian09 [15] program. The molecules were visualized using GaussView [15] and Chem3D (Cambridge-Soft, Cambridge, MA) programs. Root mean square deviations were calculated by superposition of modelled over experimental structure using Maestro program [16]. The selected topological parameters were calculated with the help of AIM2000 program [17].

## 3. Results and discussion

### 3.1. Synthesis

*N*-Ac-Mur-OMe (**1**) was prepared starting from commercially available *N*-acetyl-D-glucosamine [8]. The transformation of amide **1** to carbamate **2** was performed following the literature procedure [7]. The reaction initiated by action of  $\text{Boc}_2\text{O}/\text{DMAP}$  ( $\sim 3.3$  eq.) under reflux was completed by stirring at room temperature leaving crude imide *N*-Ac-*N*-Boc-Mur-OMe which was *in situ* treated with hydrazine hydrate (4 eq.) to give *N*-Boc-Mur-OMe (**2**) (Scheme 1).

### 3.2. IR and NMR spectroscopy

Conformational analysis of novel compound **2** in solution was performed by IR and NMR spectroscopy. Since IR spectrum contains two distinct sets of NH frequencies above and below  $\tilde{\nu} = 3400$   $\text{cm}^{-1}$ , the presence of both free and hydrogen-bonded NH groups is indicated. Hydrogen bonding is additionally supported with low-energy  $\text{CO}_{\text{ester}}$  vibration around  $\tilde{\nu} = 1730$   $\text{cm}^{-1}$  as a result of its hydrogen-bond-accepting ability. In order to determine if associated NH groups are engaged in intra- or intermolecular manner, IR spectra were measured within the concentration range  $c = 5 \times 10^{-2}$  M to  $1 \times 10^{-3}$  M. The unchanged intensity ratio of the NH vibrations upon dilution strongly supports *intramolecular* hydrogen-bonding pattern (Fig. 2 and Scheme 1). These findings are compatible with those obtained for Ac-protected analogue **1** [3] suggesting that bulky Boc-group do not considerably interfere with the hydrogen-bonding (Table 2). In addition, solid-state IR spectra of both **1** and **2** contain exclusively signals of associated NH and CO groups (Fig. 2 and Table 2).

The suggested  $\text{NH}_{\text{Boc}} \cdots \text{OC}_{\text{ester}}$  IHB was elucidated by NMR spectroscopy as a useful method to estimate a hydrogen-bond-donating capacity of NH groups. Commonly, amide protons involved in hydrogen bonds are shifted above  $\delta = 7$  ppm in non-hydrogen-bonding solvents. (Owing to the fast equilibration between hydrogen-bonded and free states, proton chemical shifts represent weighted averages of the chemical shifts of all of the contributing states). In comparison with Ac-protected **1**, amide proton of Boc-protected **2** is shifted upfield in non-competitive aprotic  $\text{CDCl}_3$  ( $\delta = 6.02$  ppm) suggesting somewhat difficult involvement in hydrogen-bonding. Since changing solvent to the strong hydrogen bond acceptor DMSO (expected to induce a downfield shift of solvent-exposed NH groups but not to affect the chemical shifts of NH groups associated in intramolecular manner) did not cause

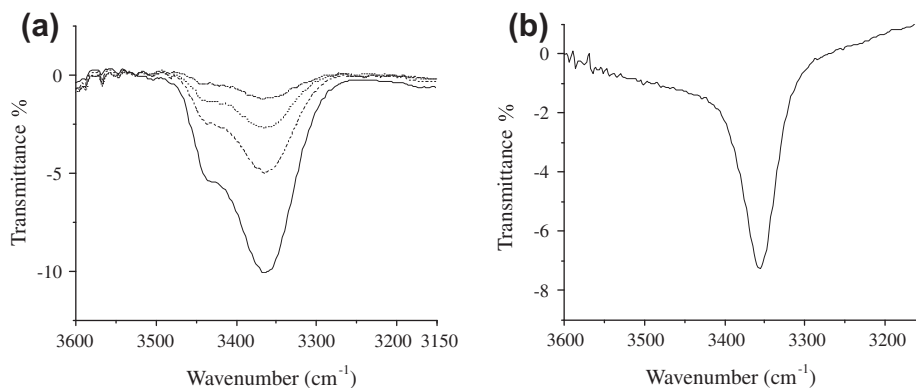


Fig. 2. The NH-stretching vibrations in concentration-dependent IR spectra of **2** in CH<sub>2</sub>Cl<sub>2</sub> (a) and KBr (b).

**Table 2**  
IR spectroscopic data [ $c = 5 \times 10^{-2}$  M in CH<sub>2</sub>Cl<sub>2</sub> and as KBr disc, (cm<sup>-1</sup>)], <sup>1</sup>H NMR data and chemical shift variation ( $\Delta\delta$ ) of the NH protons **1** [3] and **2** [ $c = 5 \times 10^{-2}$  M in CDCl<sub>3</sub> and DMSO, (ppm)].

		$\nu_{\text{NH}}$ (free)	$\nu_{\text{NH}}$ (associated)	$\nu_{\text{CO}}$ (ester)		$\delta_{\text{NH}}$	$\Delta\delta_{\text{NH}}$
<b>1</b>	CH <sub>2</sub> Cl <sub>2</sub>	3431 (w)	3356 (m)	1732 (s)	CDCl <sub>3</sub>	7.49	0.34
	CsI		3300 (m)	1737 (s)	DMSO	7.83	
<b>2</b>	CH <sub>2</sub> Cl <sub>2</sub>	3438 (w)	3365 (m)	1733 (s)	CDCl <sub>3</sub>	6.02	0.57
	KBr		3355 (m)	1728 (s)	DMSO	6.59	

significant chemical shift ( $\Delta\delta = 0.57$ ), the *IHB of medium strength* was indicated.

Whereas hydrogen-bond-assisted self-assembly of neighbouring molecules is subjected to disruption upon dilution or heating, we measured concentration- and temperature-dependent NMR spectra in order to clarify the pattern of hydrogen-bonding (intra- or intermolecular) in **2**. The chemical shifts of protons involved in intermolecular hydrogen bonds are expected to be considerably shifted upfield ( $\Delta\delta = 1 - 4$  ppm) upon heating or dilution. Since successive dilution (50–6.25 mM) did not affect the chemical shift of the amide proton (Fig. 3a), aggregation effects in CDCl<sub>3</sub> are excluded and *intramolecular* hydrogen bond is strongly supported. In addition, temperature-dependent NMR spectra, showing negligible higher-field shifting of amide protons (Fig. 3b), sustain proposed intramolecular hydrogen-bonding motif. Namely, intermolecular hydrogen bonds and hydrogen bonds to solvent undergo cleavage at increased temperatures which results in discernible upfield shifting of the related amide protons [4,18]. Conformational studies of peptides in aqueous solutions [19] and

in CDCl<sub>3</sub> [20] revealed that amide proton temperature coefficients are significantly influenced by the solvent polarity. Hence, contrary to the case of the aqueous solution, a measured large temperature dependence ( $\Delta\delta/\Delta T$ ) in non-competitive CDCl<sub>3</sub> is referred to initially shielded amide group that became exposed through dissociation of intermolecular aggregates or the disruption of intramolecular hydrogen bonds [20]. Taken into account that IR and concentration-dependent NMR analysis already excluded intermolecular aggregations, relatively large temperature dependence of examined amide proton ( $\Delta\delta/\Delta T = -6$  ppb) indicates its participation in intramolecular hydrogen bond.

### 3.3. Crystal structure

The molecular structure of *N*-Boc-Mur-OMe (**2**) determined by single crystal X-ray diffraction is shown in Fig. 4. Its stereochemistry is known from the synthesis, so determination of absolute configuration was not necessary. There is no intramolecular hydrogen bond, which was observed spectroscopically,

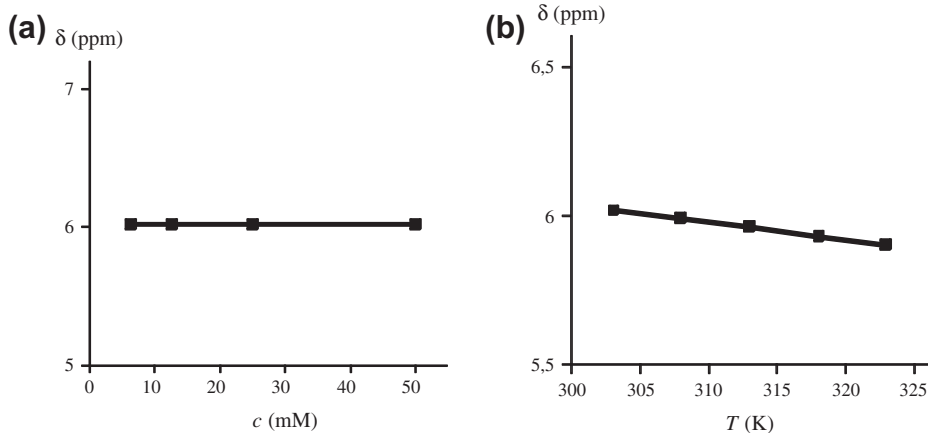
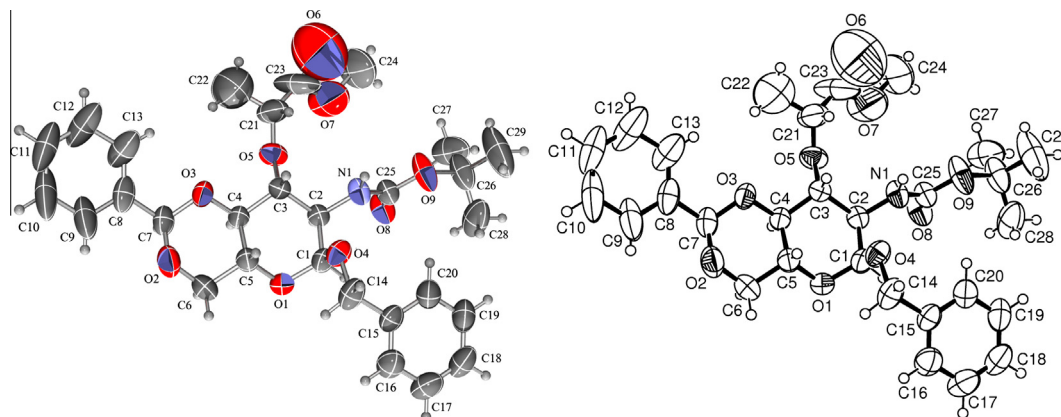


Fig. 3. (a) Concentration- and (b) temperature-dependent NH chemical shifts of **2**.



**Fig. 4.** ORTEP-3 [12] drawing of a molecule of *N*-Boc-Mur-OMe (**2**). Displacement ellipsoids are drawn for the probability of 50% and hydrogen atoms are shown as spheres of arbitrary radii.

therefore the conformation in the solid state is different than in solution. It also markedly differs from the calculated minimum-energy conformer (*vide infra*). In the crystal structure the intramolecular hydrogen bond was not observed; instead an intermolecular hydrogen bond  $\text{NH}_{\text{Boc}} \cdots \text{OC}_{\text{Boc}}$  is present. It links the molecules into chains parallel with the direction [100] (Fig. 5). Therefore, it can be argued that this hydrogen bond is responsible for the stabilisation of the conformation found in the solid state, since there are no other intermolecular interactions other than dispersion. While the solid-state conformation of the molecule itself is not an energy minimum, it can pack much more efficiently than the most stable conformer; the energy of the crystal packing (especially of intermolecular hydrogen bonding) can apparently offset the difference.

The crystals were rather poor, and the quality of the measured data was also poor, resulting with a relatively high *R* (Table 1). Displacement ellipsoids illustrate conformational flexibility of the molecule (Fig. 4), also indicating that the solid-state conformation may not be very stable. All flexible parts of the molecule (i.e. those

where free rotation about single bonds is possible) have much larger ellipsoids than the relatively rigid central part. Especially large and elongated ones belong to the Boc and methylpropanoate groups (Fig. 4), indicating a disorder. The present measurement cannot distinguish between static and dynamic disorder (i.e. many similar, but stable conformations vs. large-amplitude motion), therefore, a conformational analysis was performed by computational methods.

### 3.4. Computational study

Computational studies have already proven very useful for acquiring additional information about the geometry of the most stable conformers and for better understanding of interactions between the molecules. Some studies included research of very similar *N*-Ac-Mur-OMe (**1**) itself or coupled to the ferrocene unit [3]. Thereby, the synthesized *N*-Boc-Mur-OMe (**2**) was investigated by the means of DFT calculations with the aim to find the most sta-

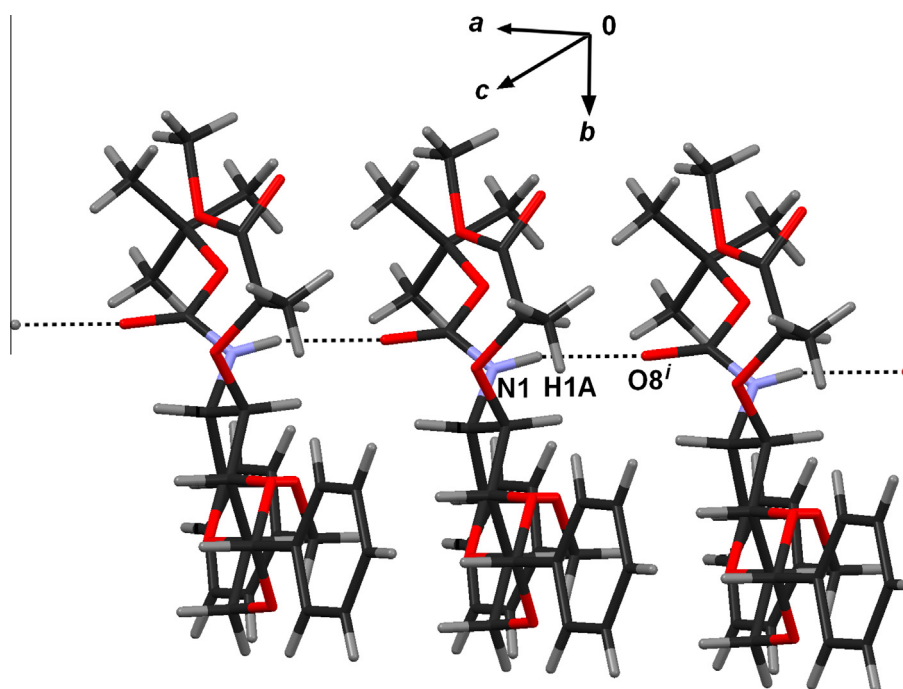


**Fig. 5.** Hydrogen bonded chain extending in the direction [100]. Parameters of the hydrogen bond:  $d(\text{N1}-\text{H1A}) = 0.86 \text{ \AA}$ ;  $d(\text{H1A} \cdots \text{O8}^i) = 2.13 \text{ \AA}$ ;  $d(\text{N1} \cdots \text{O8}^i) = 2.951(4) \text{ \AA}$ ;  $(\text{N1}-\text{H1A} \cdots \text{O8}^i) = 159^\circ$ . Symmetry operator (*i*)  $-1 + x, y, z$ .



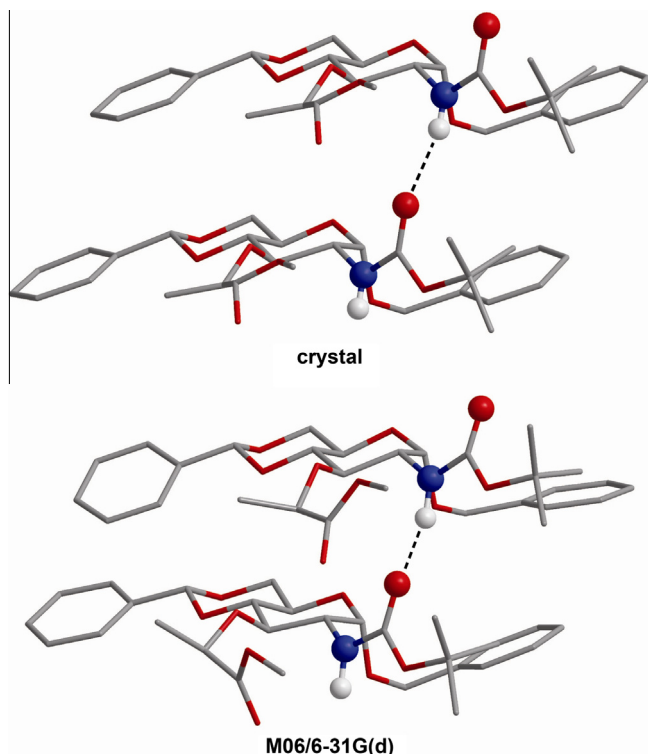


**Fig. 7.** The dimer of **2** (non-polar hydrogen atoms excluded) and its geometry optimized at M06/6-31G(d) in vacuum. The intermolecular HB is displayed.

stable conformers (approximately 50 of them) were further optimized with the Gaussian09 program. At first, the most widely accepted B3LYP functional with the 6-31G(d) basis set in vacuum was used. The reliability of the computational model was tested by comparison of two geometries. The referent geometry was monomer unit of **2** cut out from X-ray determined structure and it was compared with its optimized geometry. Upon the optimization, the major difference between these two geometries was different orientation of the phenyl groups due to their rotation. Consequently, newer functionals like M06 and M06-2X that are capable to treat dispersion interactions more adequately were decided to use. The slightly better agreement is achieved with M06 functional as it can be seen from the RMSD calculated for the non-hydrogen atoms by superposition of the optimized and the corresponding crystal geometry (monomer or dimer). The calculations were performed in vacuum and in chloroform. The data calculated for the most stable conformers are presented in Table 3 and in Fig. 6. MOL files of selected optimized geometries are available as [Supplementary files](#).

The ensembles of the most stable conformers calculated with two selected functionals (M06 and M06-2X) in vacuum and in  $\text{CHCl}_3$  have very similar distributions. All the conformers include intramolecular  $\text{NH}\cdots\text{OC}$  hydrogen bond between the carbamate nitrogen (from the amino protected group) and the carboxylic oxygen (from the carboxyl protected group) forming 8-membered ring. Several subsets of conformers were formed, depending on the torsional angles that define rotation of groups attached to the central bicyclic moiety. In all of the displayed conformers the orientation of the lactate ester group is fixed by  $\text{NH}\cdots\text{OC}$  hydrogen bond with the protected amino group. The smallest destabilization in energy arises from the different position of the Boc-protecting group, which is determined by the value of H–N–C–O dihedral angle – **M1**, **M3** and **M5** (around  $170^\circ$ ), **M2** and **M4** (around  $-10^\circ$ ). For example, this difference between two sets of the conformers (**M1** and **M2**, **M3** and **M4**) calculated at M06/6-31G(d) is

approximately  $0.30 \text{ kJ mol}^{-1}$  in  $\text{CHCl}_3$  and  $0.03 \text{ kJ mol}^{-1}$  in vacuum. More pronounced destabilization is the consequence of the phenyl and benzyloxy groups rotations as it can be seen in Fig. 6 and in Table 3. For example, the relative energy difference between **M1** and **M3** conformers with different orientations of phenyl group is approximately  $1.20 \text{ kJ mol}^{-1}$  in  $\text{CHCl}_3$  and  $2.04 \text{ kJ mol}^{-1}$  in vacuum. All the intramolecular hydrogen bonds were verified according to the suggested Koch and Popelier criteria [21] based on the topological properties (like electron density and Laplacian of the electron density) at the bond critical point between the hydrogen and hydrogen bond acceptor atom. The calculated values are in the range of 0.022–0.034 a.u. for electron density,  $\rho(r)$ , and 0.0714–0.0745 for Laplacian of the electron density,  $\nabla^2\rho(r)$ , which is also confirmation of hydrogen bond presence. The slightly large values correspond to the hydrogen bond of the conformers **M1** and **M3** with the H $\cdots$ O distance of 2.00 Å and the N–H–O angle of  $162^\circ$ . For comparison, conformers **M2** and **M4**, with different torsional angle describing rotation around (H)N–C(O) bond, have H $\cdots$ O distance of 2.02 Å and the N–H–O angle of  $158^\circ$ .

Previously described approach with one monomer unit is probably adequate for the description of the intramolecular interactions in solution, mainly hydrogen bonds. This is also supported by spectroscopic data, as it was already shown in preceding chapters. At the same time, the non-existence of the intramolecular hydrogen bond in the X-ray structure, prompted the idea to investigate the energetics associated with the crystal packing of monomer units. The simplest model for the crystal structure was used. The dimer unit consisted of two monomer units connected by the intermolecular hydrogen bond were cut out from the crystal structure and optimized in vacuum at the same level of theory previously used for the monomer unit optimization, i.e. M06/6-31G(d). These two geometries are shown in Fig. 7. The accompanied RMSD value of 0.657 was determined for non-hydrogen atoms. The interaction energy was calculated as the energy difference between the energy of dimer and twice the energy of the monomer. In this way calculated interaction energy might have the inherent error known as Basis Set Superposition Error (BSSE), so the correction by the counterpoise method (CP) is usually needed [22–24]. The calculated interaction energy is around  $-123 \text{ kJ mol}^{-1}$  ( $-61 \text{ kJ mol}^{-1}$  with included BSSE correction) what implies considerable stabilisation as a consequence of favourable interactions (mainly intermolecular hydrogen bond) between two monomer units. The accompanied deformation of the monomer units, which resulted from crystal packing, was calculated as the energy difference between the

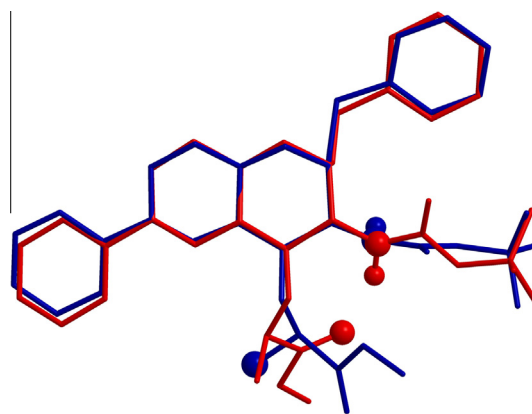


**Fig. 8.** The superposition of optimized X-ray monomer unit (blue colour, without IHB) over the similar most stable conformer of **2** (red colour, with IHB) optimized at M06/6-31G(d). The non-polar hydrogen atoms are not displayed. (For interpretation of the references to colour in this figure legend, the reader is referred to the web version of this article.)

energy of each monomer it acquired in dimer and the energy of the most stable conformer calculated with the same computational model. The corresponding changes in energy are approximately  $19 \text{ kJ mol}^{-1}$  for the monomer unit containing hydrogen bond acceptor atom and  $33 \text{ kJ mol}^{-1}$  for the other monomer unit with the hydrogen bond donor atom included. These energetically unfavourable deformations were obviously largely overcome by the energy gained through the favourable intermolecular interactions, mostly hydrogen bonds. Alternatively, the energy gained from the intramolecular hydrogen bond formation in one monomer was roughly estimated as the energy difference of two optimized geometries shown in Fig. 8. The energy of the conformer **M1** (with IHB) is about  $17 \text{ kJ mol}^{-1}$  lower than the energy of the conformer (without IHB) optimized starting from the geometry of monomer unit initially cut out from crystal structure. Using these simplified models, it was demonstrated that intermolecular or intramolecular hydrogen bonds notably contribute in stabilization of the investigated system. Using these simplified models, it was demonstrated that intramolecular hydrogen bond could also stabilize compound **2** (e.g. in solution) in the absence of the intermolecular hydrogen bond (crystal lattice).

#### 4. Conclusions

The aim of this work was to examine if the structural properties of fully protected derivatives of biologically important muramic acid are influenced by the protecting groups incorporated into its N-terminus. Therefore, the novel *N*-Boc-Mur-OMe (**2**), prepared by transformation of *N*-Ac-Mur-OMe (**1**), was subjected to conformational analysis in solution by using concentration-dependent IR as well as concentration- and temperature-dependent NMR-spectroscopy. The obtained values were compared to those resulted from spectroscopic measurements of previously described Ac-analogue **1** revealing that 8 membered  $\text{NH}\cdots\text{OC}_{\text{ester}}$  intramolecular hydrogen bond was preserved upon alteration of protecting group. However, changing solvent to the hydrogen bond acceptor (DMSO) caused larger downfield chemical shift for Boc-analogue **2** ( $\Delta\delta = 0.57$ ), indicating its weaker hydrogen-bonding activity in comparison with Ac-analogue **1** ( $\Delta\delta = 0.34$ ). Computational studies included combination of molecular and quantum mechanical calculations in vacuum and in solvent (PCM). Among the selected computational models, M06/6-31G(d) provided the best agreement between the calculated and the X-ray determined geometry. The conformational analysis of *N*-Boc-Mur-OMe (**2**) in chloroform corroborated the experimental data from measurements in solution and confirmed the existence of the intramolecular  $\text{NH}\cdots\text{OC}_{\text{ester}}$  hydrogen bond involved in 8-membered ring. The calculated interaction energy of two monomers in vacuum indicated the considerable stabilisation from the intermolecular hydrogen bond formed between the monomers. Solid-state *N*-Boc-Mur-OMe (**2**) exhibited quite different structural pattern based on intermolecular hydrogen bonds: the hydrogen bond donor is the same as in solution state, but the hydrogen bond acceptor of the  $\text{NH}\cdots\text{OC}$  is the carbonyl oxygen belonging to a different molecule, resulting in infinite hydrogen-bonded chains. While the conformation in the solid state is less stable than those observed in solution (as confirmed by quantum chemical calculations), it is apparently favoured by intermolecular interactions.

#### Acknowledgments

This research was supported by the Ministry of Science, Education and Sports of the Republic of Croatia (Grant Numbers 058-1191344-3122, 119-1191342-1339 and 098-1191344-2943).

The computational resources provided by Isabella cluster (isabella.srce.hr) at the Zagreb University Computing Centre (SRCE) were used for this research.

#### Appendix A. Supplementary material

Supplementary crystallographic data for this paper can be obtained free of charge via [www.ccdc.cam.ac.uk/conts/retrieving.html](http://www.ccdc.cam.ac.uk/conts/retrieving.html) (or from the Cambridge Crystallographic Data Centre, 12, Union Road, Cambridge CB2 1EZ, UK; fax: +44 1223 336033; or deposit@ccdc.cam.ac.uk). CCDC923167 contains the supplementary crystallographic data for this paper. Supplementary data associated with this article can be found, in the online version, at <http://dx.doi.org/10.1016/j.molstruc.2013.06.011>. These data include MOL files and InChIKeys of the most important compounds described in this article.

#### References

- [1] (a) S. Traub, S. von Aulock, T. Hartung, C. Herrmann, J. Endotoxin Res. 12 (2006) 69; (b) M.V. Pashenkov, S.F. Popilyuk, B.I. Alkhozova, V.L. L'vov, V.V. Murugin, E.S. Fedenko, R.M. Khaitov, B.V. Pinegin, Int. Immunopharmacol. 10 (2010) 875; (c) C. Werts, L. le Bourhis, J. Liu, J.G. Magalhaes, L.A. Carneiro, J.H. Fritz, S. Stockinger, V. Balloy, M. Chignard, T. Decker, D.J. Philpott, X. Ma, S.E. Girardin, Eur. J. Immunol. 37 (2007) 2499; (d) Y.C. Yoo, K. Yoshimatsu, Y. Koike, R. Hatsuse, K. Yamanishi, O. Tanishita, J. Arikawa, I. Azuma, Vaccine 16 (1998) 216; (e) D. Stewart-Tull, Annu. Rev. Microbiol. 34 (1980) 311; (f) A. Adam, V. Souvannavong, E. Lederer, Biochem. Biophys. Res. Commun. 85 (1978) 684.
- [2] L. Barišić, M. Rošćić, M. Kovačević, M. Čakić Semenčić, Š. Horvat, V. Rapić, Carbohydr. Res. 346 (2011) 678.
- [3] C. Förster, M. Kovačević, L. Barišić, V. Rapić, K. Heinze, Organometallics 31 (2012) 3683.
- [4] L. Barišić, M. Kovačević, M. Mamić, I. Kodrin, Z. Mihalić, V. Rapić, Eur. J. Inorg. Chem. 11 (2012) 1810.
- [5] G.A. Dilbeck, L. Field, A.A. Gallo, R.J. Gargiulo, J. Org. Chem. 43 (1978) 4593.
- [6] J.M. Burk, J.G. Allen, J. Org. Chem. 62 (1997) 7054.
- [7] C. Henry, J.-P. Joly, Y. Chapleur, J. Carbohydr. Chem. 18 (1999) 689.
- [8] (a) A. Babić, S. Pečar, Tetrahedron-Assymetr. 19 (2008) 2265; (b) P.H. Gross, M. Rimpler, Liebigs Ann. Chem. 1 (1986) 37.
- [9] Oxford Diffraction, CrysAlis PRO, Oxford Diffraction Ltd., 2007.
- [10] G.M. Sheldrick, Acta Crystallogr. A 64 (2008) 112.
- [11] A.L. Spek, J. Appl. Cryst. 36 (2003) 7.
- [12] L.J. Farrugia, J. Appl. Cryst. 30 (1997) 565.
- [13] C.F. Macrae, P.R. Edgington, P. McCabe, E. Pidcock, G.P. Shields, R. Taylor, M. Towler, J. van de Streek, J. Appl. Cryst. 39 (2006) 453.
- [14] (a) MacroModel, version 9.8, Schrödinger, LLC, New York, NY, 2010; (b) F. Mohamadi, N.G.J. Richards, W.C. Guida, R. Liskamp, M. Lipton, C. Caufield, G. Chang, T. Henrickson, W.C. Still, J. Comput. Chem. 11 (1990) 440.
- [15] (a) M.J. Frisch, G.W. Trucks, H.B. Schlegel, G.E. Scuseria, M.A. Robb, J.R. Cheeseman, G. Scalmani, V. Barone, B. Mennucci, G.A. Petersson, H. Nakatsuji, M. Caricato, X. Li, H.P. Hratchian, A.F. Izmaylov, J. Bloino, G. Zheng, J.L. Sonnenberg, M. Hada, M. Ehara, K. Toyota, R. Fukuda, J. Hasegawa, M. Ishida, T. Nakajima, Y. Honda, O. Kitao, H. Nakai, T. Vreven, J.A. Montgomery Jr., J.E. Peralta, F. Ogliaro, M. Bearpark, J.J. Heyd, E. Brothers, K.N. Kudin, V.N. Staroverov, R. Kobayashi, J. Normand, K. Raghavachari, A. Rendell, J.C. Burant, S.S. Iyengar, J. Tomasi, M. Cossi, N. Rega, J.M. Millam, M. Klene, J.E. Knox, J.B. Cross, V. Bakken, C. Adamo, J. Jaramillo, R. Gomperts, R.E. Stratmann, O. Yazyev, A.J. Austin, R. Cammi, C. Pomelli, J.W. Ochterski, R.L. Martin, K. Morokuma, V.G. Zakrzewski, G.A. Voth, P. Salvador, J.J. Dannenberg, S. Dapprich, A.D. Daniels, Ö. Farkas, J.B. Foresman, J.V. Ortiz, J. Cioslowski, D.J. Fox, Gaussian 09, Revision A.02, Gaussian Inc., Wallingford, CT, 2009; (b) R. Dennington, T. Keith, J. Millam, GaussView 5.0, Wallingford, CT, 2009.
- [16] Maestro, Version 9.1, Schrödinger, LLC, New York, NY, 2011.
- [17] (a) F. Biegler-König, J. Schömbohm, D.J. Bayles, J. Comp. Chem. 22 (2001) 545; (b) F. Biegler-König, J. Schömbohm, J. Comp. Chem. 23 (2002) 1489.
- [18] T.K. Chakraborty, A. Ghosh, R. Nagaraj, A. Ravi Sankar, A.C. Kunwar, Tetrahedron 57 (2001) 9169.
- [19] T. Cierpicki, J. Otlewski, J. Biomol. NMR 21 (2001) 249.
- [20] E.S. Stevens, N. Sugawara, G.M. Bonora, C. Toniolo, J. Am. Chem. Soc. 102 (1980) 7048.
- [21] (a) U. Koch, P.L.A. Popelier, J. Phys. Chem. 99 (1995) 9747; (b) P.L.A. Popelier, J. Phys. Chem. A 102 (1998) 1873.
- [22] H.B. Jansen, P. Ros, Chem. Phys. Lett. 3 (1969) 140.
- [23] S. Simon, M. Duran, J.J. Dannenberg, J. Chem. Phys. 105 (1996) 11024.
- [24] S.F. Boys, F. Bernardi, Mol. Phys. 19 (1970) 553.